J Bioenerg Biomembr (2010) 42:55–67
DOI 10.1007/s10863-009-9267-x

# Mitochondrial bioenergetic adaptations of breast cancer cells to aglycemia and hypoxia

**Katarína Smolková · Nadège Bellance · Francesca Scandurra · Elisabeth Génot · Erich Gnaiger · Lydie Plecitá-Hlavatá · Petr Ježek · Rodrigue Rossignol**

Received: 19 October 2009 / Accepted: 2 December 2009 / Published online: 19 January 2010


**Abstract** Breast cancer cells can survive and proliferate under harsh conditions of nutrient deprivation, including limited oxygen and glucose availability. We hypothesized that such environments trigger metabolic adaptations of mitochondria, which promote tumor progression. Here, we mimicked aglycemia and hypoxia in vitro and compared the mitochondrial and cellular bioenergetic adaptations of human breast cancer (HTB-126) and non-cancer (HTB-125) cells that originate from breast tissue. Using high-resolution respirometry and western blot analyses, we demonstrated that 4 days of glucose deprivation elevated oxidative phosphorylation five-fold, increased the spread of the mitochondrial network without changing its shape, and decreased the apparent affinity of oxygen in cancer cells (increase in $C_{50}$), whereas it remained unchanged in control cells. The substrate control ratios also remained constant following adaptation. We also observed the Crabtree effect, specifically in HTB-126 cells. Likewise, sustained hypoxia (1% oxygen during 6 days) improved cell respiration in non-cancer cells grown in glucose or glucose-deprived medium (+ 32% and +38%, respectively). Conversely, under these conditions of limited oxygen or a combination of oxygen and glucose deprivation for 6 days, routine respiration was strongly reduced in cancer cells (−36% in glucose medium, −24% in glucose-deprived medium). The data demonstrate that cancer cells behave differently than normal cells when adapting their bioenergetics to micro-environmental conditions. The differences in hypoxia and aglycemia tolerance between breast cancer cells and non-cancer cells may be important when optimizing strategies for the treatment of breast cancer.

**Keywords** Mitochondria · Oxidative phosphorylation · Breast cancer · Tumor bioenergetics · Hypoxia · Respirometry

**Abbreviations**

| | |
|---|---|
| ADP | adenosine diphosphate |
| ANT | adenine nucleotide translocator |
| ATP | adenosine triphosphate |
| COX | cytochrome c oxidase |
| Cyt c | cytochrome c |
| CoQ | coenzyme Q |
| ETS | electron transport system |
| OXPHOS | oxidative phosphorylation |

K. Smolková · N. Bellance · R. Rossignol
INSERM U688,
Bordeaux, France

K. Smolková · N. Bellance · R. Rossignol (✉)
Université Victor Segalen Bordeaux 2,
Bordeaux, France
e-mail: rossig@u-bordeaux2.fr

F. Scandurra
OROBOROS INSTRUMENTS,
Innsbruck, Austria

E. Génot
INSERM U889, IECB,
Pessac, France

E. Gnaiger
Department of General and Transplant Surgery, D. Swarovski Research Laboratory, Medical University of Innsbruck,
Innsbruck, Austria

K. Smolková · L. Plecitá-Hlavatá · P. Ježek
Institute of Physiology, Dept. 75,
Academy of Sciences of the Czech Republic,
Prague, Czech Republic

## Introduction

Understanding how cancer cells derive their vital energy from microenvironmental nutrients and oxygen is of fundamental importance for the development of anti-cancer therapies and diagnostic approaches (Kroemer & Pouyssegur 2008). Recent developments indicate that the bioenergetic features of cancer cells are highly variable and could reflect both the primitive metabolic processes of cancer-initiating cells and their ongoing modulation by the tumor microenvironment (Ježek et al. 2009). The Warburg hypothesis (Warburg 1930) of glycolytic-only cancer cells was recently challenged by biochemical studies that revealed the existence of a wide class of tumors where ATP is produced at a higher extent by mitochondrial oxidative phosphorylation (OXPHOS) rather than solely by glycolysis (Moreno-Sanchez et al. 2007). Hence, a survey of these studies showed that various tumors generate a significant part of their ATP (> 80%) by the mitochondrion (Zu & Guppy 2004). An effort has been made in the last decade to propose a bioenergetic classification of cancer cells according to the relative contribution of glycolysis and OXPHOS to the cellular ATP supply (Moreno-Sanchez et al. 2007). This effort has been supported by molecular studies designed to decipher the metabolic profile of various types of cancer cells and have provided evidence for a bioenergetic signature of human tumors (Cuezva et al. 2004; Cuezva et al. 2002). Yet, the determination of the expression level of key components of glycolysis and OXPHOS could be used for molecular diagnostics and prognostics. Additional detailed investigations of the OXPHOS system in tumors revealed a broader range of modifications including decreased mitochondrial biogenesis (Bellance et al. 2009a; Cuezva et al. 1997; Pedersen 1978), alterations in the activity of respiratory chain complexes (Simonnet et al. 2002; Simonnet et al. 2003), inhibition of the pyruvate dehydrogenase (PDH) complex (Kim et al. 2006), truncation of the Kreb's cycle with citrate extrusion (Hatzivassiliou et al. 2005), tighter binding of hexokinase II to the mitochondrion (Pedersen 2007), changes in organellar shape and size (Arismendi-Morillo 2009; Arismendi-Morillo & Castellano-Ramirez 2008) and the accumulation of mutations in mitochondrial DNA (Chatterjee et al. 2006; Ishikawa et al. 2008). These studies (see review article (Bellance et al. 2009b)) helped to delineate the metabolic remodeling of cancer cells and inspired further investigations. It remains unknown whether the metabolic profile of cancer cells originates from a predetermined cancer initiating stem cell or how the tumor microenvironment molds the pattern. In a previous study, we showed that both the type and the availability of energy substrates participate in the determination of a cancer cell's bioenergetic profile (Rossignol et al. 2004). For instance, glucose deprivation led to a profound modification of energy pathways toward oxidative metabolism with upregulation of respiratory chain proteins and higher branching along with constriction of the mitochondrial network in uterine cervix adenocarcinoma (HeLa), osteosarcoma (143B) and hepatocellular carcinoma (HEPG2) (Plecitá-Hlavatá et al. 2008; Rossignol et al. 2004). Such aglycemia-driven changes were less evident in non-cancer cells, suggesting a cancer specific adaptability to bioenergetic stresses (Rossignol et al. 2004). It is also well known that human primary cells excised from their tissue of origin and placed in cell culture dishes for artificial growth rapidly shift toward a glycolytic phenotype (Gnaiger & Kemp 1990; Gstraunthaler et al. 1999). Besides glucose, another key player in the definition of a cancer cell's metabolic profile is oxygen tension ($p_{O2}$). Hypoxia is a common feature of the microenvironment of cancer cells, and tumor oxygenation can be severely compromised as compared to normal tissue (Vaupel et al. 2007). Thus, it seems more appropriate to investigate the impact of hypoxia and aglycemia on cancer cells, which typically encounter this type of stress in situ. Therefore, we focused our study on breast cancer cells, which have the adaptive capacity to survive under such microenvironmental substrate deprivation (Vaupel & Hockel 2000). Indeed, Vaupel and coworkers observed low values for intratumoral oxygen tension ranging between 3 to 10 mmHg in breast malignant tissue while non-cancer tissue exhibited higher values approximating 50 mmHg (Vaupel et al. 2003). The "Gatenby and Gillies" microenvironmental model of carcinogenesis (Gatenby & Gillies 2004; Gatenby & Gillies 2008) considers that pre-cancer cells are typically found in tissue regions where oxygen and glucose delivery is low. This might have pre-adapted energy metabolism to a life of uncontrolled growth and deregulated cell death. They further proposed that during tumor growth, angiogenesis leads to the growth of inadequate microvasculature, which results in intermittent oxygen and glucose deprivation in cancer cells along with acidification of the extracellular space. Although the impact of aglycemia, hypoxia and acidification on cancer cell metabolic remodeling was analyzed in parcellar studies, their combined interaction was insufficiently investigated. Different levels of hypoxia are observed in tumors, and Vaupel proposed the "Janus face" model whereby metabolic adaptations are thought to occur when oxygen levels decrease below 1%, while more drastic hypoxia (below 0.1%) could trigger the generation of new genetic variants and resistance to apoptosis (Vaupel 2008; Vaupel & Mayer 2005). In the present study, we conducted a longitudinal bioenergetic analysis of oxygen and glucose deprivation in human breast carcinoma cells (HTB-126) and breast non-cancer cells (HTB-125).

Our results suggest a bioenergetic improvement of the mitochondrial system in cancer cells after 6 days of growth in the absence of glucose. Conversely, hypoxia at 1% $O_2$ triggered a large reduction in OXPHOS capacity, which resulted in cell death when growth was not supported by glycolysis. This demonstrates that cancer cells behave differently than normal cells in bioenergetic adaptations to microenvironmental conditions.

## Materials and methods

*Cell types and culture conditions* HTB-126 (cell strain derived from the ductal carcinoma of the breast) and HTB-125 (control cell line originating from the same patient, a normal fibroblast-like line from normal breast tissue peripheral to the infiltrating ductal carcinoma, which was the source of HTB-126) were purchased from ATCC. The 'glucose medium' consisted of High Glucose Dulbecco's Modified Eagle Media (DMEM; GIBCO, No 11995), containing 25 mM glucose, supplemented with 10% fetal calf serum (*Hyclone*), 10 mM HEPES, 100 U/ml penicillin and 100 U/ml streptomycin. Alternatively, we used 'galactose medium' that consisted of DMEM without glucose (GIBCO, No 11966), supplemented with galactose (10 mM final), glutamine (6 mM final), 10 mM HEPES, 1 mM sodium pyruvate, 100 U/ml penicillin, 100 U/ml streptomycin and 10% dialyzed fetal calf serum (*Hyclone,* No SH30079). All cells were kept in 5% $CO_2$ at 37 °C at air saturation. Hypoxia was obtained by growing the cells in a dedicated hypoxic chamber (In vivo 300 from Biotrace International) with 5% $CO_2$ and a controlled mixture of air/$N_2$ to achieve stable 1% $O_2$.

*Cell viability* We used the neutral red assay to assess cell viability, as originally described in (Borenfreund & Puerner 1985). Cells were grown in 96-well plates under various conditions including aglycemia and hypoxia. Cells were washed with 0.9% NaCl and incubated with 1/60 *v/v* of a 4 mg/ml neutral red solution for 2 h at 37 °C. Cells were then washed with 0.9% NaCl and fixed by rapidly washing with a formol-calcium solution (1 ml formaldehyde 40%, 10 ml of 10% calcium-chloride and 89 ml distilled water). Once fixed, cells were permeabilized and their intracellular membranes lysed with a solution of 50% ethanol and 1% acetic acid; this results in the extraction of neutral red from the cell. Finally, the mixtures were homogenized by stirring the plate. Absorbance was measured in a multi-well scanning spectrophotometer (SAFAS MP96) at a wavelength of 540 nm with a reference wavelength of 630 nm. Tests were performed in quadruplicates, and each set was repeated three times. The results of neutral red uptake (viability) were expressed as a percent of the control (untreated cells) absorbance.

*Respirometry* Mitochondrial oxygen consumption assays were performed using the high-resolution respirometry system Oxygraph-2 k (OROBOROS INSTRUMENTS, Austria). This instrument provides sufficient sensitivity and time resolution for analysis of the kinetics of oxygen during mitochondrial and cellular respiration (Gnaiger 2001). Cell respiration was measured at different cell densities (from $2{\cdot}10^5$ to $2{\cdot}10^6$ per ml according to volume-specific flux) at 37 °C in 2-ml chambers containing culture medium (DMEM) at a stirring rate of 750 rpm. Data were digitally recorded using DatLab4 software; oxygen flux was calculated as the negative time derivative of the oxygen concentration, $c_{O2}(t)$. Oxygen sensors were calibrated routinely at air saturation and in oxygen depleted media. A standard correction was performed for instrumental background oxygen flux arising from oxygen consumption of the oxygen sensor and minimum back-diffusion into the chamber. Two types of polarographic investigations were performed: a) flux measurement on intact cells (as described in (Hutter et al. 2004)), and b) oxygen kinetics with $c_{50}$ (or $p_{50}$) determination (as described in (Pecina et al. 2004; Steinlechner-Maran et al. 1996)). For the oxygen kinetics measurements, the respiration rate was recorded continuously along the entire oxygen range with a data recording interval of 1 s. The data were corrected for the response time of the oxygen sensor (usually 3–5 s (Gnaiger 2001)). $c_{50}$ and $J_{max}$ values were determined in the 1.1 kPa (about 10 µM) oxygen range using a standard algorithm provided in DatLab2 software (Gnaiger et al. 1995). The apparent $c_{50}$ is the oxygen concentration for the half-maximum respiration measured on intact cells under a given condition. It provides a measure of the limitation of mitochondrial energy production by oxygen availability (Gnaiger et al. 1998). The factor for conversion of oxygen pressure to oxygen concentration is 9.5 ($O_2$ solubility in DMEM [µM × $kPa^{-1}$]).

In our study, we determined various bioenergetic parameters that characterize the cellular state of aerobic energy production (Gnaiger 2008). ROUTINE respiration (*R*) was measured in intact cells in a given culture medium (e.g., glucose or galactose) in the coupled state of physiological respiratory control. Non-coupled resting respiration, or LEAK respiration (*L*), is obtained in the presence of oligomycin (2 µg/ml), which inhibits the mitochondrial phosphorylation system so that no ATP can be produced, and electron flow reflects the energy requirement to compensate for the proton leak. The maximal uncoupled respiratory activity measured in the presence of optimum uncoupler concentration (0.5 µM steps, 1.5 µM FCCP final concentration in our study) provides a measure of the kinetic capacity of the electron transport system, or ETS capacity (*E*), under conditions of physiological substrate supply in the intact cell. Using the

ETS capacity as a common basis for normalization of coupling control ratios, the *R/E* reflects the level of mitochondrial activity relative to the maximal kinetic capacity of the electron transport system. Correspondingly, the *L/E* ratio reflects the level of LEAK respiration relative to the ETS capacity and provides an estimate of intrinsic uncoupling. Finally, the fraction of respiration actually used for ATP production is estimated as the difference of *R/E-L/E* or (*R-L)/E* (Hutter et al. 2004). The Crabtree effect was studied by addition of glucose (25 mM final concentration in high-glucose medium) to galactose medium. Respiration of permeabilized cells was measured in respiration medium MiR05 (0.5 mM EGTA, 3 mM $MgCl_2.6H_2O$, 65 mM KCl, 20 mM taurine, 10 mM $KH_2PO_4$, 20 mM HEPES, 110 mM sucrose and 1 g/l BSA, pH 7.1). Respiratory substrates were 2 mM malate, 10 mM glutamate for Complex I respiration, with addition of 10 mM succinate to determine the additive effect of convergent electron input through Complex I + II (Gnaiger 2009). OXPHOS capacity was measured with 4 mM ADP. Respiration was inhibited with rotenone (200 nM), antimycin A (2.5 μM) or KCN (0.5 mM).

*Microscopy* The morphology of the mitochondrial network was studied by fluorescence confocal microscopy using Mitotracker Green (Invitrogen) 150 nM for 20 min at 37 °C, on a FluoView laser scanning inverted microscope (Nikon). The objective used was a Plan Apochromat 60.0X/1.4/0.21 oil spring loaded. The images were aquired using the EZ-C1 Gold Version 3.2 build 610, as follow (at 37 °C): the pinhole was set at 33.3 μm and the image size was 1024×1024. The step size was 0.5 μm, and the aquisition time of the Z-series set at 10 frames per second. The number of images was adapted to the width of each cells determined individually. The reconstitution of the three-dimensional images was performed using Imaris Software (Bitplane). Cells were grown in glucose or glucose-deprived medium, in normoxia or hypoxia (as precised in the results and legends) on glass chamber (Lab-Tek chamber slides: 2 wells (glass) of 4.2 $cm^2$ per well; ref. 177380) and series of images were taken from three different chambers. 100 images per experimental condition (HTB-125 or HTB-126; glucose or galactose) were selected randomly, and the analysis was performed using a double-blinded approach. The area of mitochondrial sections was determined on the projections made from each series of images. The size of the mitochondrial compartment was evaluated with the morphometric software "Morpho. Pro" by Explora Nova (France). It allowed to select automatically the region of interest (*i.e* the mitochondrial network or the nucleus), and to calculate the area occupied by the selected pixels.

*Western-Blotting* Cell lysis was performed using 4% lauryl-maltoside, for 30 min on ice. Sample preparation and electrophoresis were performed as described previously (Benard et al. 2006). Antibody against the respiratory chain complexes were obtained from *Mitoscience* (Eugene, OR). Actin antibody were purchased from *SantaCruz Biotechnology*; The signal were detected using the chemiluminescent ECL Plus reagent (GE Healthcare) and a Chemidoc system (Biorad). It was quantified by densitometric analysis using Image J (*NIH*) software.

*Statistical analysis* All the data presented in this study correspond to the mean value of *N* experiments ± SD, with $N \geq 3$ (see figure legends). Comparison of the data sets was performed with the Student's *t* test, using SigmaPlot. Two sets of data were considered statistically different when $P<0.05$.

## Results

*1) Cell viability is supported by OXPHOS in glucose-deprived medium* Breast cancer cells (HTB-126) and non-cancer cells (HTB-125) were grown in cell culture medium with or without glucose, as previously described (Reitzer et al. 1979; Rossignol et al. 2004). The neutral red assay measures the active uptake of neutral red inside the cell. It can be used as a metabolic index related to cell viability, as discussed previously (Nouette-Gaulain et al. 2009). To assess the actual dependency of neutral red uptake on mitochondrial energy production, we first determined the effect of inhibitors of the OXPHOS system (Fig. 1). The results indicate a dose-dependent inhibition of the neutral red uptake by $F_1$-$F_0$ ATP synthase inhibitor oligomycin (Fig. 1a), Complex I inhibitor rotenone (Fig. 1b) and Complex III inhibitor antimycin A (Fig. 1c) in HTB-126 cancer cells grown in galactose-glutamine medium. No significant effect was observed for the same doses of inhibitors in HTB-126 cells grown in glucose medium (Fig. 1a, b, c). This demonstrates that cancer cells' viability is closely linked to mitochondrial energy production in glucose-deprived medium.

*2) The viability of cancer cells is controlled by glucose distribution and oxygen availability* The effect of hypoxia was studied while cells were incubated at normoxia or hypoxia (1% oxygen) during 1 or 6 days, and cell viability was assessed using the neutral red assay during the exponential phase of growth in glucose or galactose-glutamine medium (Fig. 1d). We expressed the results as the ratio of the neutral red uptake measured in hypoxia to that measured at normoxia. A ratio of 1 indicates that viability was similar in hypoxia and normoxia; a ratio < 1 indicates a loss of viability in hypoxia. In HTB-125 non-cancer cells grown in glucose medium, hypoxia reduced cell viability at day one (20±14% reduction), and no

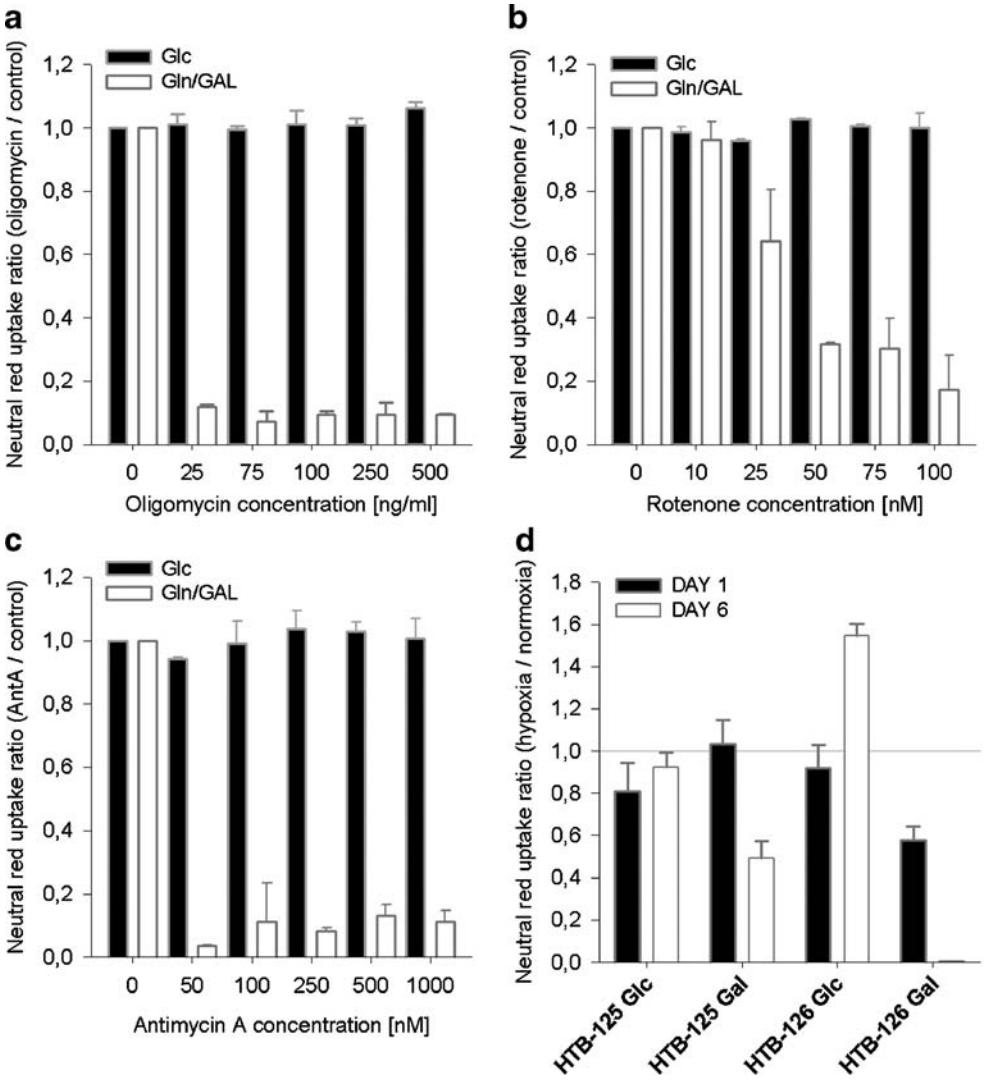


**Fig. 1** Cell viability. Effect of mitochondrial inhibition on cell viability of cancer cells HTB-126 grown in glucose medium (HTB-126 Glc) and in glucose-deprived medium (HTB-126 Gal) in the presence of mitochondrial inhibitors oligomycin (**a**), rotenone (**b**), and antimycin A (**c**) incubation for 8 hours, measured by the neutral red assay. Data are expressed as the ratio of the neutral red uptake measured in cells treated with OXPHOS inhibitors to that obtained in absence of inhibitors. Values are means ± SD with $N$=3. (**d**) Cell viability of HTB-125 and HTB-126 grown in glucose (Glc) or glucose-deprived (Gln/Gal) medium under normoxia (21% $O_2$) and hypoxia (1% $O_2$). Data are expressed as neutral red uptake ratios of normoxic to hypoxic cells at day 1 (black) and 6 (white) in 1% oxygen. Values are means ± SD. $N$=5

significant change was detected at day six. Conversely, in cancer cells (HTB-126), 6 days of hypoxia resulted in a large increase in cell viability (54±6% increase). In glucose-deprived medium, 6 days of hypoxia resulted in a significant decrease of cell viability both in HTB-125 cells (51±8% reduction after 6 days) and in cancer HTB-126 (all the cells died). This suggests that 6 days of growth at 1% $O_2$ hypoxia exerts opposite effects on cancer cell viability depending on the presence or absence of glucose in the culture medium.

*3) Sustained glucose deprivation improves OXPHOS capacity in cancer cells* We used high-resolution respirometry to assess the impact of glucose deprivation on ROUTINE respiration in intact cells (Fig. 2a). We compared the respiratory activities obtained a) in glucose medium, b) just after glucose removal and replacement by galactose-glutamine (indicated by the symbol "Gal 0"), and c) after 4 days of growth in glucose-deprived medium (indicated by the symbol "Gal 4"). ROUTINE respiration in glucose medium was lower ($P$<0.05) for the HTB-126 cancer cells ($JO_2$=24±4.8 pmol $O_2 \cdot s^{-1} \cdot 10^{-6}$ cells) versus the HTB-125 non-cancer cells ($JO_2$=41.4±1.6 pmol $O_2 \cdot s^{-1} \cdot 10^{-6}$ cells). The immediate removal of glucose ("Gal 0") produced no significant effect in non-cancer cells, while a doubling of the respiratory activity was measured in cancer cells (Fig. 2a). This increase is known as the removal of the Crabtree effect, which describes glucose-mediated instant suppression of respiration. In another set of experiments, we measured cell respiration after 4 days of growth in galactose medium (Fig. 2a). We observed a large increase ($P$<0.05) of ROUTINE respiration in cancer cells (90.7±4.8 pmol $O_2 \cdot s^{-1} \cdot 10^{-6}$ cells), but no significant change ($P$<0.05) was measured in non-cancer cells (49.9±4.4 pmol $O_2 \cdot s^{-1} \cdot 10^{-6}$ cells). Under all conditions, we also determined the oxygen pressure at 50% of maximum flux ($c_{50}$), which gives a measure of the apparent affinity of the cell for oxygen (see traces of Fig. 2b). The $c_{50}$ was a constant 0.6 to 0.8 μM in HTB-125 cells under all substrate conditions (Glc, Gal 0 and Gal 4; Fig. 2c) when respiratory activity was unchanged (Fig. 2a).

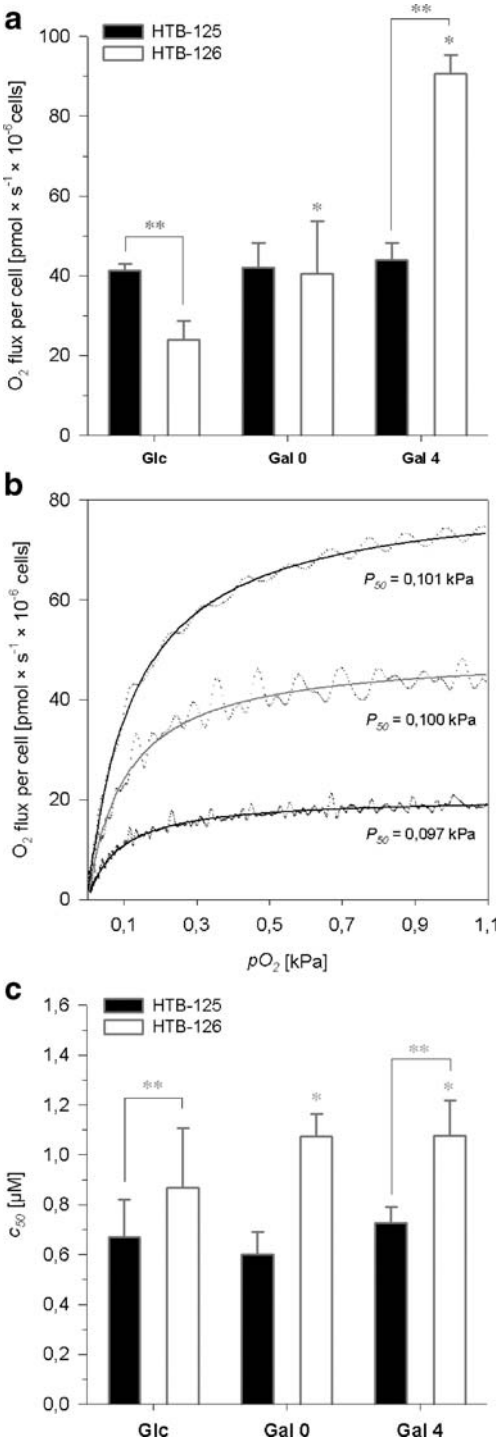


**Fig. 2** Cell respiration in glucose/glucose-deprived medium. (**a**) ROUTINE respiration of HTB-125 and HTB-126 cells in glucose (Glc), after glucose removal (Gal 0) and grown in glucose-deprived medium (Gal 4). Values are means ± SD. *$P$<0.05 glucose-deprived compared to glucose; **$P$<0.05 cancer cell line (HTB-126) compared to control cell line (HTB-125). Values are means ± SD with $N$>5. (**b**) Cell specific respiratory flux as a function of $p_{O2}$ of cancer HTB-126 cells in glucose medium (lower lines), after glucose removal (middle line) and in galactose medium (upper line). Representative traces of $10^6$ cells/ml in culture medium. Dots represent single data points. Data recording interval was 1 s. Solid lines represent hyperbolic fit calculated in the low-oxygen range <1.1 kPa. (**c**) Influence of cultivation conditions on cell respiration of normal and breast cancer cells—$c_{50}$. $c_{50}$ of HTB-125 and HTB-126 cells in glucose (Glc), after glucose removal (Gal 0) and grown in glucose-deprived medium (Gal 4). Values are means ± SD. $N$>5. * $P$<0.05 glucose-deprived compared to glucose; ** $P$<0.05 cancer cell line (HTB-126) compared to control cell line (HTB-125)

This $c_{50}$ value agrees with the oxygen affinity observed in human umbilical vein endothelial cells and fibroblasts (Pecina et al. 2004; Steinlechner-Maran et al. 1996)). The $c_{50}$ increased significantly to 1.1 µM (affinity to oxygen decreased) in HTB-126 cells (Gal 4) when respiration per cell doubled in comparison to HTB-125 cells (Fig. 2). Such an increase in $c_{50}$ is expected with an increasing turnover of cytochrome $c$ oxidase (Gnaiger et al. 1998). However, it was surprising that the $c_{50}$ did not decline in HTB-126 cells in the presence of glucose under conditions of suppressed respiration (Fig. 2c). The constant $c_{50}$, therefore, indicates a regulatory mechanism related to the Crabtree effect, the nature of which has not been resolved.

*4) Short-term glucose deprivation illustrates the reversibility of the Crabtree effect* While considering the peculiarities of the bioenergetics of HTB-126 cancer cells, one must distinguish adaptive features (such as the enhancement of cell respiration observed only after 4 days of growth in glucose-deprived medium; see above) from negative properties. The Crabtree effect does not require that adaptations occur, and it was previously defined as the inhibition of mitochondrial ATP production by high concentrations of glucose in yeast (Crabtree 1928) and subsequently in cancer cells. We observed such a control of OXPHOS by glucose in the HTB-126 cancer cells, since the addition of glucose ("Glc") to these cells grown in glucose-deprived medium ("Gal0") triggered a large (39%, $P$<0.05) reduction in cell respiration (Fig. 3a). This phenomenon was fully rescued when cells grown in glucose medium were shifted to a glucose-deprived medium (Fig. 3b). This Crabtree effect was also observed on the uncoupled flux of respiration (Fig. 3c), indicating that inhibition by glucose was not mediated by glycolytic phosphorylation of ADP to ATP. Hence, our data reveal a kinetic inhibition of the electron transport system by glucose in cancer cells. This effect was not observed in the non-cancer HTB-125 cells (data not shown). The $c_{50}$ remained unchanged when the Crabtree effect was removed. After 4 days of growth in glucose-deprived medium ("Gal4"), adaptations occurred and ROUTINE respiration increased (Fig. 3a).

*5) Long-term glucose deprivation leads to increased cell respiration without a change in R/E and L/E coupling control ratios or Complex I/Complex II utilization* The actual state of mitochondrial respiration in culture medium

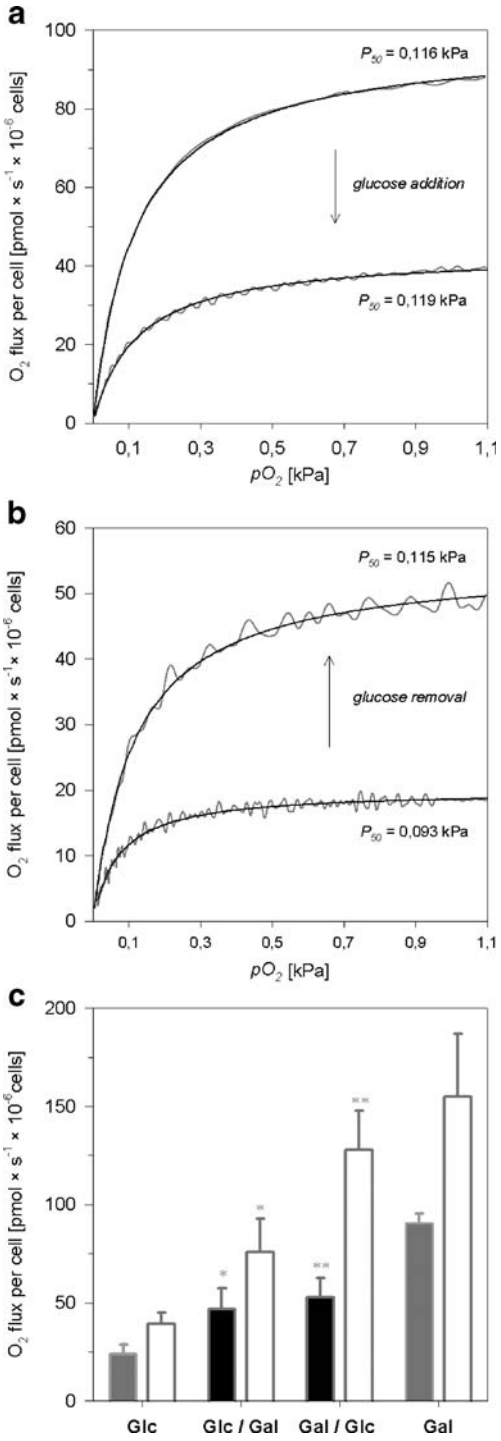


**Fig. 3** Crabtree effect in breast cancer cells. Effect of glucose addition (**a**) and glucose removal (**b**) on ROUTINE respiration of intact cells expressed as cell-specific oxygen flow per $10^6$ cells as a function of $p_{O2}$. Corresponding $p_{50}$ values are shown in the graph. (**c**) Respiration of cancer cells upon glucose addition and removal, comparison of ROUTINE respiration (full bars) and ETS capacity of uncoupled respiration (empty bars) per $10^6$ cells. Cells grown in glucose medium (Glc), after glucose removal (Glc/Gal), grown in glucose deprived medium (Gal) and after glucose addition to cells grown in glucose-deprived conditions (Gal/Glc). Values are means ± SD. $N>5$. *$P<0.05$ of Glc/Gal group compared to Glc group; **$P<0.05$ Gal/Glc group compared to Gal group

can be determined in intact cells by the evaluation of two parameters: the *L/E* coupling control ratio, which reflects the extent of intrinsic uncoupling, and the *R/E* coupling control ratio, which expresses the ROUTINE respiration relative to the maximal electron transport system (ETS) capacity. The fraction of oxygen consumption used for ATP production is the (*R-L)/E* ratio (see Methods). In HTB-125 non-cancer cells, we observed a significantly lower *L/E* ratio (0.07±0.02) as compared to the HTB-126 cancer cells (0.17±0.07) (Fig. 4a). This demonstrates an exacerbated proton leak in cancer cells, which did not vary significantly upon glucose removal in the two cell types. The *R/E* ratio was higher ($P<0.05$) in cancer cells (0.51±0.05) as compared to non-cancer cells (0.40±0.05), indicating a lower apparent excess capacity of ETS in cancer cells. Yet, the (*R-L*)/*E* ratios presented no difference between the two cell types, nor after glucose removal (Fig. 4a), suggesting a compensation for the partial uncoupling in cancer cells such that the ETS capacity was used at the same extent to produce ATP. Moreover, specific substrates and inhibitors can be used in permeabilized cells to describe the respiratory system. In HTB-126 cells previously grown in glucose medium or adapted to long-term growth in glucose-deprived medium, we observed a similar increase in cell respiration when the energy substrates for Complex I respiration (glutamate + malate) were complemented by addition of succinate for determination of convergent Complex I + II respiration (Fig. 4b). The constant substrate control ratios demonstrate that the entire respiratory system was upregulated upon adaptation to glucose-deprivation, which suggests an activation of mitochondrial biogenesis in response to sustained glucose deprivation.

*6) Glucose deprivation stimulates the expression of OXPHOS proteins in cancer cells* The expression levels of respiratory chain proteins (subunits of complex I, complex II and complex IV) were analyzed by western blots of cell lysates prepared from HTB-125 and HTB-126 cells grown in glucose medium ("Glc") or glucose-deprived medium for 4 days ("Gal4"). An example of a western blot is given in the inset of Fig. 4c, and the results of the densitometric analysis (performed under non-saturating conditions; see inset of Fig. 4c) are summarized in the histogram. We expressed the ratios of the protein band densities measured in samples from glucose-deprived medium to those obtained in glucose medium (for the same content of cell lysate proteins). A value of 1 signifies no change in the expression level of Complex II, IV and I in glucose-deprived medium while a value >1 indicates an upregulation of these proteins. The results show an increase

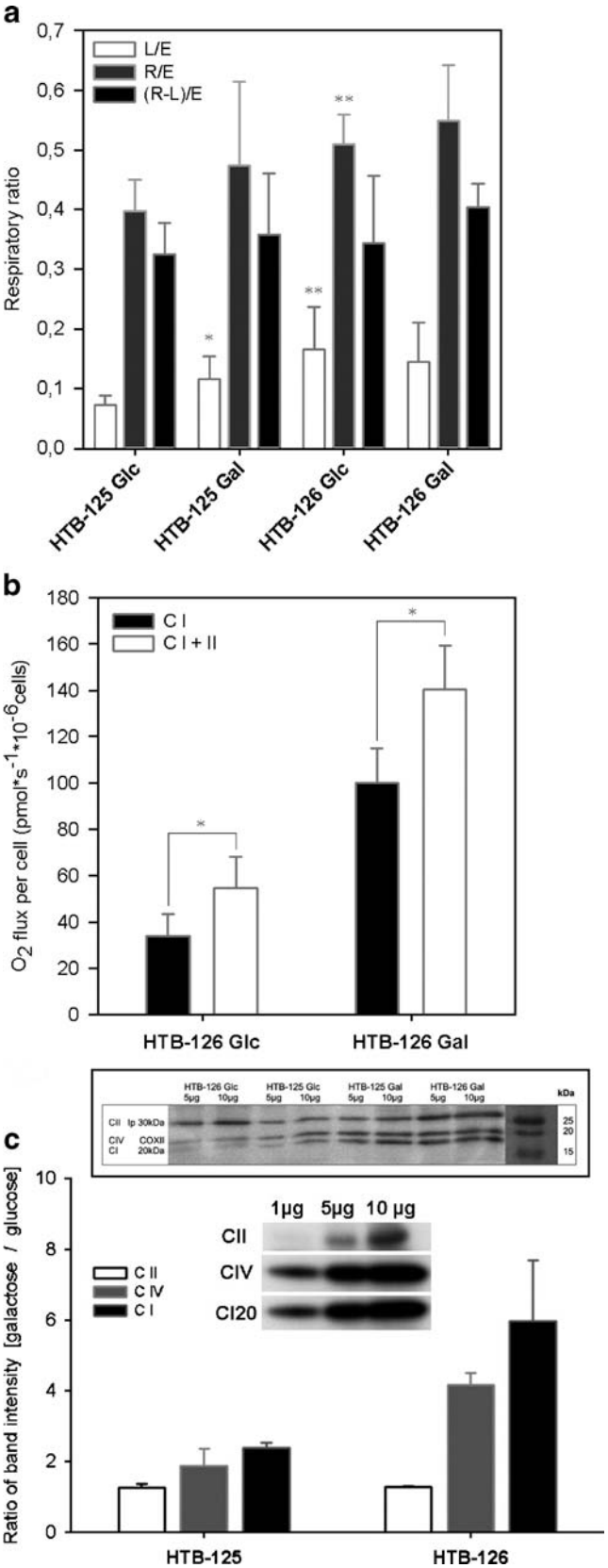


**Fig. 4** Respiratory ratios of HTB-125 and HTB-126 intact cells Glc vs. Gal; components of cell respiration in intact cells. (**a**) Respiratory ratios calculated from polarographic measurements on intact cell using substrates present in the growth medium, and some inhibitors. *L/E* ratio (white bars) was calculated as the oligomycin-inhibited respiratory rate (LEAK respiration, *L*) over the maximal respiratory rate obtained with an uncoupler (ETS capacity, *E*); *R/E* ratio (grey bars) was calculated as the ROUTINE respiratory rate (*R*) over the maximal respiratory rate (*E*); and (*R-L*)/*E* ratio gives the fraction of respiration that is used under routine conditions to produce ATP. Values are means ± SD. *N*>5. (**b**) State 3 respiration of Complex I (CI) and Complex I + II (CI + II) of permeabilized cells, quantified by addition of substrates glutamate and malate (CI) and succinate-rotenone (CI + II) in the presence of ADP. Values are means ± SD. *N*>5. (**c**) Western-blot quantification of the respiratory chain content of normal and breast cancer cells upon glucose deprivation. Contents of respiratory Complexes I, II and IV were determined using whole cell lysates of HTB–125 and HTB–126 cells grown in glucose or glucose-deprived medium. Results are expressed as ratios of band intensities normalized to beta-actin of the corresponding glucose-deprived to glucose sample pairs. Band intensity was quantified by densitometry. Values are means ± SD *N*=3. *Graph inset (top)* shows an exemplar western–blot; note band designation and molecular weight (kDa, number in right). *Graph inset (bottom*) shows the verification for non-saturating conditions for the three antibodies used (CI, CII and CIV). * $P<0.05$ glucose-deprived compared to glucose; ** $P<0.05$ cancer cell line (HTB-126) compared to control cell line (HTB-125)

($P<0.05$) of protein expression levels with a mean factor of 1.26±0.098, 1.88±0.48 and 2.39±0.15 for CII, CIV and CI in non-cancer cells grown in the absence of glucose, respectively. In cancer cells, this increase was more pronounced, and the mean factor values were of 1.28± 0.01, 4.17±0.34 and 5.97±1.7 for CII, CIV and CI, respectively. These data evidence a stronger induction of OXPHOS protein expression in cells deprived of glucose.

*7) Contrary effects of oxygen limitation on mitochondrial respiration in cancer cells versus non-cancer cells* The ROUTINE cell-specific respiration of HTB-125 and HTB-126 cells grown in glucose or glucose-deprived medium for prolonged time (full adaptation is reached after 4 days) was measured after 6 days in normoxia or 1% hypoxia, as was the pH value of the cell culture medium (Fig. 5). In non-cancer cells grown in glucose medium, 1% $O_2$ hypoxia significantly enhanced cell respiration measured at normoxia ($P<0.05$), by 34% after 6 days. This reflects the increased capacity of the respiratory system. This phenomenon was also observed in glucose-deprived medium (26% increase). Conversely, in cancer cells, 1% $O_2$ hypoxia led to a reduction of routine respiration measured in normoxia in both glucose medium and glucose-deprived medium (36% and 24% reduction, respectively). The pH measurement revealed a significant ($P<0.05$) acidification of the medium by cancer cells grown under aglycemia and hypoxia. This finding argues for a different sensitivity and a variable response of cell energy metabolism toward hypoxia in cancer in comparison to non-cancer cells.

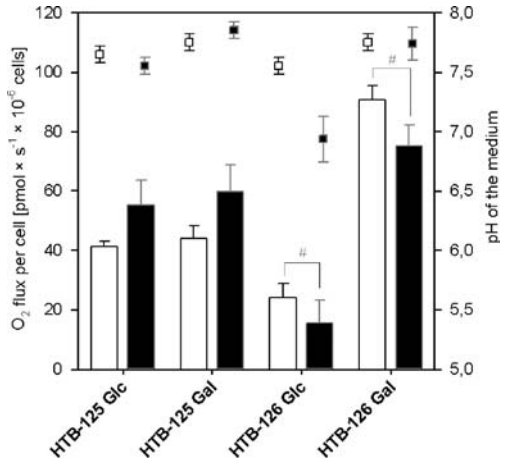


**Fig. 5** Effect of hypoxia on respiratory flux and medium pH of normal and breast cancer cells. Respiratory flux of intact HTB-125 and HTB-126 cells in glucose (Glc) or glucose-deprived medium (*Gal*) in normoxia (open columns) and after exposure to 1% $O_2$ for 6 days (full columns) expressed as a cell-specific flow per $10^6$ cells (Y1 axis). #$P<0.05$. pH of the culture medium was measured after cultivation (Y2 axis). Symbols and bars are means ±SD; $N=3$

*8) Determination of mitochondrial network morphology and area in breast cancer and non-cancer cells* Mitochondrial bioenergetic capacity is intimately linked to the configuration of the mitochondrial network in physiology (Benard et al. 2007; Plecitá-Hlavatá et al. 2008; Rossignol et al. 2004) and pathology (Willems et al. 2009); therefore, we analyzed this feature in living HTB-125 and HTB-126 cells by confocal microscopy (Fig. 6). In non-cancer HTB-125 cells, neither the removal of glucose nor the limitation of oxygen availability separately triggered a change of the mitochondrial network morphology and total area. The histogram in Fig. 6 summarizes the results of the morphometric analysis performed on HTB-125 and HTB-126 cells after 6 days under hypoxia or aglycemia ($N\geq100$ cells were analyzed for each condition). Interestingly, the combination of aglycemia and 1% $O_2$ hypoxia induced a wider spreading of this network, as evidenced by the significant increase in the total organellar area (by a factor of 1.93 as compared to normoxic HTB-125 in glucose medium). In HTB-126 cancer cells, these changes were more sensitive since the sole removal of glucose triggered an increase in mitochondrial total area (by a factor of 1.51). Yet, the combination of aglycemia and 1% $O_2$ hypoxia induced further changes (the total mitochondrial area was increased by a factor of 1.91) comparable to those observed in non-cancer HTB-125 cells. In all conditions, the mitochondrial network remained in the tubular configuration, and no excessive fragmentation was observed (data not shown).

## Discussion

In order to study the bioenergetic adaptation of breast cancer cells and its consequences on cell viability, we mimicked in vitro the tumor microenvironmental conditions of tumor oxygen limitation (less than 1% $O_2$; $p_{O2}$ < 7 mmHg or 1 kPa) and glucose deprivation (no glucose; replaced by galactose and glutamine (Reitzer et al. 1979; Rossignol et al. 2004)). In HTB-126 cancer cells and HTB-125 non-cancer cells, we assessed mitochondrial oxidative capacity and affinity for oxygen after one and 6 days of hypoxia, aglycemia or a combination of both stresses.

Prior to the analysis of cancer cell bioenergetic adaptation to environmental substrate limitations, it was necessary to study the mitochondrial respiratory capacity of cancer cells and non-cancer cells. To this end, we compared the rate of respiration of these cells placed in the same conditions of energy substrate availability, pH and temperature. In glucose medium, the rate of respiration was lower for cancer cells as compared to non-cancer cells. We concluded that mitochondrial respiratory capacity is reduced in cancer cells. However, the rate of ROUTINE respiration of cancer cells measured in the absence of glucose ("Gal 0" conditions) was similar to that of non-cancer cells. This discrepancy is known as the Crabtree effect, which states that high concentrations of glucose inhibit mitochondrial respiration in cancer cells. In our study, we demonstrate the reversibility of this phenomenon in breast cancer cells. The underlying mechanisms still remain unresolved, and current theories suggest that some intermediates of glucose oxidation could inhibit mitochondrial oxidative phosphorylation. Biochemical studies performed on yeast suggest that fructose 1,6-bisphosphate could play a determining role in this process (Diaz-Ruiz et al. 2008). Hepatoma cells show a 50-fold increase in this metabolite concentration following 5 mM glucose addition to the cells (Rodriguez-Enriquez et al. 2001). Interestingly, addition of galactose did not change the level of fructose 1,6-bisphosphate in that study, and we observed the removal of this Crabtree effect when glucose was replaced by galactose. It is important to note that galactose is not used as a fuel by cancer cells but serves for nucleic acid synthesis, while glutamine is consumed by the mitochondria to produce ATP. This phenomenon was demonstrated in HeLa cells or in CHO cells using $C_{13}$-labeled glucose and glutamine (Donnely & Scheffler 1976; Reitzer et al. 1979). Thus, to compare the bioenergetic status of cancer cells and non-cancer cells while taking into consideration the Crabtree effect, it is essential to compare the cells while in the "Glc" and the "Gal 0" conditions, as defined in our study. Moreover, the rapid loss of HTB-126 cancer cell viability induced by various inhibitors of the OXPHOS system was observed only in glucose-deprived medium, further emphasizing the fact that ATP is derived from OXPHOS in this medium.

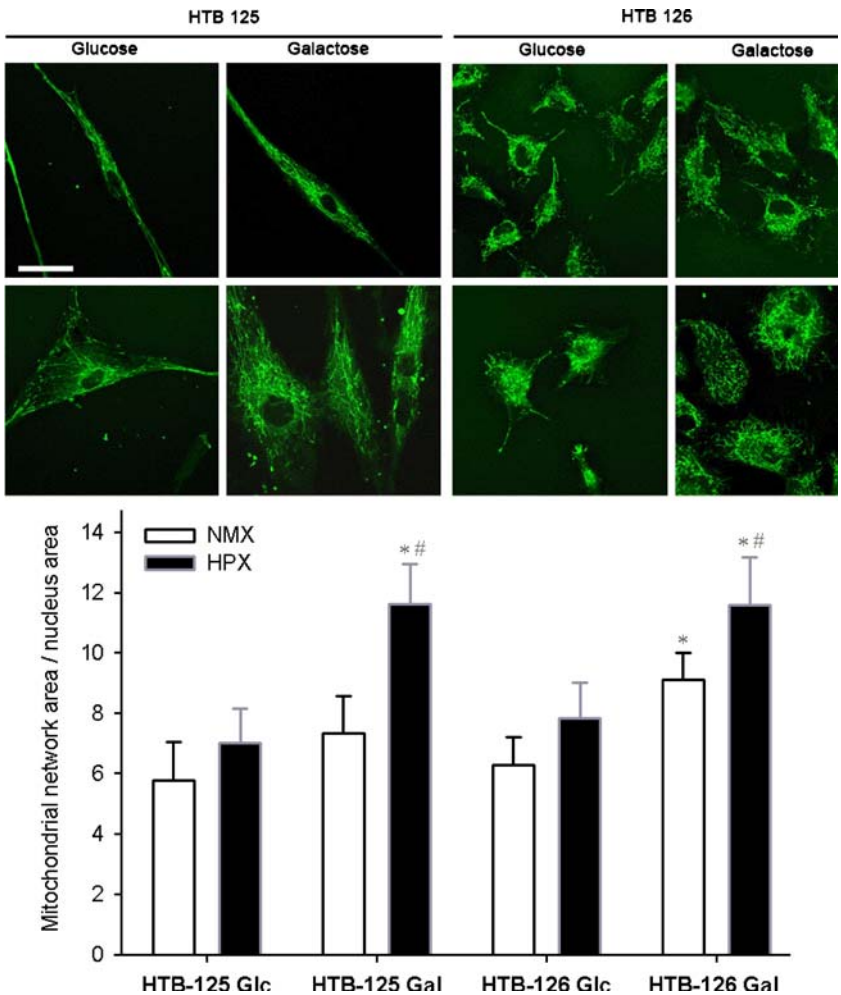


**Fig. 6** Mitochondrial network in HTB-125 and HTB-126 in normoxia and hypoxia for 6 days. Images obtained by confocal microscopy were analyzed using Morpho Pro (Explora Nova). The total mitochondrial area (green) and the nucleus area (black) were measured on 3D projections, and the ratio mitochondria/nucleus was expressed as the normalized mitochondrial compartment. * $P<0.05$ Glc compared to Gln for the same cell type, # $P<0.05$ normoxia compared to hypoxia. Values are means ± SD. $N=100$

Yet, the measurement of intact cell respiration (ROUTINE respiration) is not sufficient to delineate the bioenergetic status, since it provides no information on the actual extent of oxygen consumption used for ATP synthesis. This information is reflected more directly by the *L/E*, the *R/E* and the (*R-L*)/*E* ratios. Accordingly, we evidenced a) a more extensive proton leak in cancer cells (which might be explained by a difference in membrane composition and fluidity or slipping of the OXPHOS components), b) a lower apparent excess capacity of ETS in cancer cells (which can be explained by an upregulation of routine respiration to compensate for the increased leak) and c) the same extent of ETS utilization for ATP production. These findings might allow us to reconsider or refine the hypothesis of dysfunctional mitochondria in tumors (John 2001; Warburg 1930), as they indicate that a significant part (app. 35%) of mitochondrial respiration is used for ATP synthesis in both cell types, and the OXPHOS system plays an important role for energy production and cell survival in situations of glucose limitation. This observation strengthens the need for a thorough evaluation of the metabolic profile of tumors, along with a characterization of their microenvironment, in order to derive adapted therapies (Bellance et al. 2009b; Moreno-Sanchez et al. 2007; Zu & Guppy 2004).

Our study further demonstrates the decisive role of mitochondrial OXPHOS in cancer cell energetics, as we observed a significant upregulation of OXPHOS proteins in glucose-deprived medium. For instance, the expression level of Complex IV subunit one was increased by a factor of six after only 4 days of growth in aglycemia, and this phenomenon was associated with a three-fold increase in respiration in the HTB-126 cancer cells, yet no significant change was measured in the corresponding non-cancer cells. We also observed a significant increase (+30%) in the mitochondrial and nucleus areas in HTB-126 cancer cells grown under aglycemic conditions for 4 days, an effect that was not observed in HTB-125. This result suggests a stimulation of mitochondrial biogenesis induced by glucose deprivation, specifically in the cancer cells, in agreement with a previous study (Rossignol et al. 2004). Given the higher energy needs of cancer cells for supporting their deregulated growth and extensive biosyntheses, one could hypothesize that cancer cells must enhance their OXPHOS system when the fuel for energy production switches from glycolytic to oxidative-only. Under non-

stringent conditions, glucose is the preferential energy substrate of cancer cells, and its consumption is typically enhanced by the expression of more rapid isoforms of the glycolytic pathway (Mathupala et al. 1997). In our study, we observed the enhancement of the OXPHOS pathway when glucose was replaced by glutamine. This result indicates that the strong energy demand of cancer cells dictates the upregulation of whatever energy pathway is used, as determined by the type and availability of the energy substrate. This peculiarity has been observed for other cancer cells (HeLa, 143B (Rossignol et al. 2004) and HepG2 (Plecitá-Hlavatá et al. 2008)) and could designate the underlying pathway of metabolic remodeling as a potential target for anti-cancer therapy. These regulatory pathways could involve HIF1α, PGC-1α, and c-myc which are the main orchestrators of the pseudo-hypoxic metabolic changes (Bratslavsky et al. 2007; King et al. 2006; Pollard et al. 2005) and the energy-dependent control of mitochondrial biogenesis (Ventura-Clapier et al. 2008) and glutaminolysis (Gao et al. 2009), respectively. In addition to glucose deprivation, which drives the aforementioned metabolic adaptations, cancer cells are also confronted with oxygen limitation. Thus, we looked at the bioenergetic changes triggered by 1% $O_2$ hypoxia in HTB-126 and HTB-125 cells. We found that 1% $O_2$ hypoxia caused a 30% reduction of mitochondrial respiration (measured at normoxia) in HTB-126 cancer cells, while it induced a 30% increase in HTB-125 non-cancer cells; these differences were explained by the downregulation and the upregulation of respiratory chain protein expression, respectively. In the same experimental conditions of combined aglycemia and hypoxia (6 days), there was an increase of the relative mitochondrial area in HTB-125 or HTB-126 cells, while respiration was increased solely in HTB-125 but decreased in HTB-126 cells. Therefore, a larger mitochondrial network might not be adequately explained by a stimulation of mitochondrial biogenesis, but it could be a consequence of changes in cell morphology induced by prolonged hypoxia (Baffert et al. 2001).

The striking difference in the response to hypoxia provides evidence of specific features of cancer cells, which might be used to derive therapeutic strategies. For instance, our observation could explain why hypoxia increases tumor cell sensitivity to glycolytic inhibitors, as we observed a metabolic shift towards this pathway for cellular energy production (Liu et al. 2002). Yet, cancer cells have developed a highly (de) regulated oxygen sensing system whereby factor HIF1α has become the target of a complex pseudo-hypoxic regulatory mechanism (Bratslavsky et al. 2007). This deregulation might alter the sensitivity of cancer cells to oxygen levels and could explain the opposite response when compared to non-cancer cells where oxygen limitation triggers the upregulation of OXPHOS (see model of Fig. 7). Such an

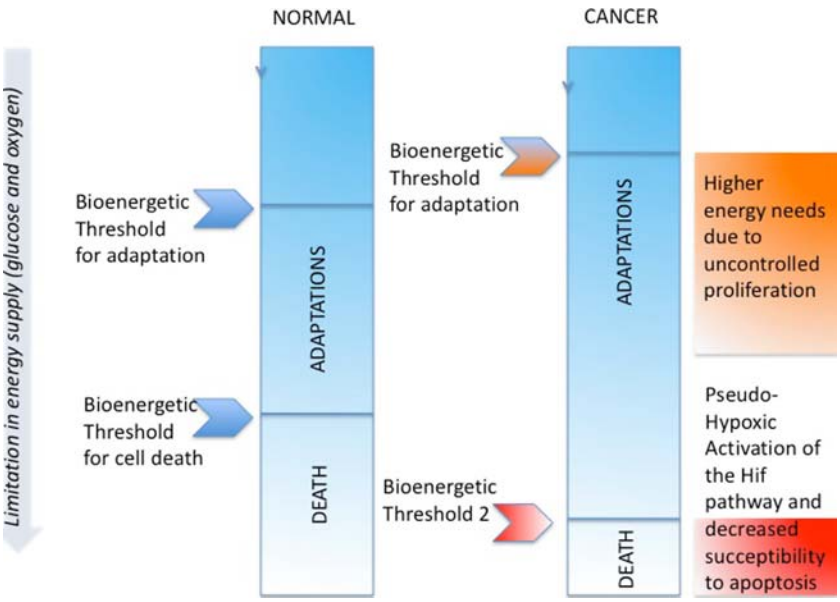


**Fig. 7** Different bioenergetic thresholds in cancer versus non-cancer cells. Cancer cells adapt their OXPHOS machinery when glucose availability is decreased, while non-cancer cells survive with less intensive adaptations. This indicates a higher sensitivity of the HTB-126 cancer cells toward glucose limitation, and this is represented by a higher "Bioenergetic threshold for adaptation" in these cells. This level of energy impairment below which OXPHOS upregulation arises determines cancer cells survival in situation of glucose deprivation. It could be explained by a high energy demand of cancer cells, and a less efficient OXPHOS system, as compared to the HTB-125. When hypoxia is combined with aglycemia, the ratio of energy demand to energy supply increases, and cancer cells die more than non-cancer cells. This is represented by a higher "Bioenergetic threshold for cell death", which indicates the limit below which a limitation of energy substrates (*e.g* glucose and oxygen together) leads to cell death. This might be explained by an already activated hypoxic sensing (pseudo-hypoxic activation of HIF) which artificially increases the sensitivity of cancer cells toward a limitation of oxygen disponibility

enhancement of OXPHOS is a compensatory, adaptive response typically observed in normal tissues and has been described in physiological conditions of hypoxia such as exercise training or high altitude (Dufour et al. 2006; Essop 2007). In our study, we observed a lower sensitivity of mitochondrial respiration toward a decrease in oxygen concentration, i.e., we measured higher $c_{50}$ values (lower apparent affinity to oxygen) in HTB-126 cells as compared to HTB-125 cells. Again, this result might be related to the existence of an interfering pseudo-hypoxic regulatory pathway in cancer cells. To complete our analysis, we combined glucose deprivation with oxygen limitation to analyze the bioenergetic adaptations that may occur, since tissue nutrient deprivation due to inadequate blood supply occurs very early during tumor development. We observed that the specific downregulation of OXPHOS triggered by hypoxia in cancer cells did no longer occur when glutamine was the only substrate for growth, i.e., when ATP can only be produced by mitochondria. Hence, under conditions of increased mitochondrial energy demand, 1% $O_2$ hypoxia cannot downregulate the OXPHOS system as occurs in glucose medium. This observation suggests that cancer cells' metabolic apparatus ultimately comprises interactions and coordination between nutrient sensing and oxygen sensing. Our observations could explain, at least in part, the existence of two classes of tumors, a glycolytic class and an OXPHOS class, as proposed previously (Bellance et al. 2009b; Moreno-Sanchez et al. 2007; Zu & Guppy 2004). In non-cancer cells, glucose-deprivation did not change the stimulatory effect of hypoxia, and OXPHOS remained intact after 6 days of growth in 1% $O_2$. Of note, stimulation of OXPHOS by glucose deprivation hypoxia was additive in cancer cells. The changes observed in our study demonstrate a profound remodeling of cancer cells' metabolic profile by energy substrate limitation, and our cell viability analysis revealed the importance of these modifications for tumor progression. Hypoxia alone greatly improved cancer cell viability in glucose medium (+54%), while it killed these cells in the absence of glucose. Hence, sustained hypoxia stimulates cell metabolism, possibly via the upregulation of glycolysis and consequent enhancement of glucose oxidation. Numerous studies showed that sustained hypoxia stabilizes the transcription factor HIFα, which activates the expression of more rapid and irreversible glycolytic genes with downstream proliferative and anabolic effects (Denko 2008). In HTB-125 non-cancer cells, no improvement of cell viability was observed after 6 days of hypoxia, which indicates that cancer cells can improve their growth under hypoxia. In glucose-deprived medium, 1% $O_2$ hypoxia killed all cancer cells and strongly reduced cell viability in HTB-125 non-cancer cells (-51%). This finding further demonstrates that cancer and non-cancer cells rely on glycolysis to survive under 1% $O_2$ hypoxia. Thus, hypoxia without glucose deprivation allows one to distinguish cancer cells from non-cancer cells with regard to differences in their metabolic adaptive capacities. This observation emphasizes the need for a better fundamental description of the pathways involved in the concertedness between oxygen sensing and nutrient sensing in cancer cells. These mechanisms will reveal important differences between cancer and non-cancer cells that could be targeted to inhibit cancer cells' metabolic adaptations and subsequent survival under conditions of glucose and oxygen limitation. The metabolic adaptation evidenced in our study might be a hallmark of most cancer cells regardless of the tissue of origin. Indeed, the upregulation of OXPHOS and the shape changes of the mitochondrial network induced by aglycemia have been observed in other cancer cells of strikingly different tissue origin: HeLa (uterine cervix), 143B Osteosarcoma (bone), INS1-E (pancreas) and HepG2 (liver) (Plecitá-Hlavatá et al. 2008; Rossignol et al. 2004). Accordingly, a recent report revealed that cancer cells lose their tissue-specific features in regards to the regulation of energy metabolism, which becomes dictated by the tumorigenic program (Acebo et al. 2009).

**Acknowledgments** We thank the French National Institute for Scientific and Medical Research (INSERM), Université Victor Segalen Bordeaux 2, Région Aquitaine, Cancéropôle Grand Sud-Ouest, CEREPEG (Registre des Tumeurs Cérébrales), Tumorothèque CHU Bordeaux, and Association contre les Maladies Mitochondriales (Ammi) for financial support. KS was supported by grants from the Academy of Sciences: No. IAA500110701 (to PJ) and AV0Z50110509. She completed a PhD thesis in "co-tutelle" between France and the Czech Republic supported by a grant from the French Government.

## References

Acebo P, Giner D, Calvo P, Blanco-Rivero A, Ortega AD, Fernandez PL, Roncador G, Fernandez-Malave E, Chamorro M, Cuezva JM (2009) Transl Oncol 2:138–145

Arismendi-Morillo G (2009) Int J Biochem Cell Biol 41:2062–2068

Arismendi-Morillo GJ, Castellano-Ramirez AV (2008) J Electron Microsc (Tokyo) 57:33–39

Baffert F, Usson Y, Tranqui L (2001) Eur J Cell Biol 80:78–86

Bellance N, Benard G, Furt F, Begueret H, Smolkova K, Passerieux E, Delage J, Baste J, Moreau P, Rossignol R (2009) Int J Biochem Cell Biol

Bellance N, Lestienne P, Rossignol R (2009b) Front Biosci 14:4015–4034

Benard G, Bellance N, James D, Parrone P, Fernandez H, Letellier T, Rossignol R (2007) J Cell Sci 120:838–848

Benard G, Faustin B, Passerieux E, Galinier A, Rocher C, Bellance N, Delage JP, Casteilla L, Letellier T, Rossignol R (2006) Am J Physiol Cell Physiol

Borenfreund E, Puerner JA (1985) Toxicol Lett 24:119–124

Bratslavsky G, Sudarshan S, Neckers L, Linehan WM (2007) Clin Cancer Res 13:4667–4671

Chatterjee A, Mambo E, Sidransky D (2006) Oncogene 25:4663–4674

Crabtree HG (1928) Biochem J 22:1289–1298

Cuezva JM, Chen G, Alonso AM, Isidoro A, Misek DE, Hanash SM, Beer DG (2004) Carcinogenesis 25:1157–1163

Cuezva JM, Krajewska M, de Heredia ML, Krajewski S, Santamaria G, Kim H, Zapata JM, Marusawa H, Chamorro M, Reed JC (2002) Cancer Res 62:6674–6681
Cuezva JM, Ostronoff LK, Ricart J, Lopez de Heredia M, Di Liegro CM, Izquierdo JM (1997) J Bioenerg Biomembr 29:365–377
Denko NC (2008) Nat Rev Cancer 8:705–713
Diaz-Ruiz R, Averet N, Araiza D, Pinson B, Uribe-Carvajal S, Devin A, Rigoulet M (2008) J Biol Chem 283:26948–26955
Donnely M, Scheffler I (1976) J cell Physiol 89:39–52
Dufour SP, Ponsot E, Zoll J, Doutreleau S, Lonsdorfer-Wolf E, Geny B, Lampert E, Fluck M, Hoppeler H, Billat V, Mettauer B, Richard R, Lonsdorfer J (2006) J Appl Physiol 100:1238–1248
Essop MF (2007) J Physiol 584:715–726
Gao P, Tchernyshyov I, Chang TC, Lee YS, Kita K, Ochi T, Zeller KI, De Marzo AM, Van Eyk JE, Mendell JT, Dang CV (2009) Nature 458:762–765
Gatenby RA, Gillies RJ (2004) Nat Rev Cancer 4:891–899
Gatenby RA, Gillies RJ (2008) Nat Rev Cancer 8:56–61
Gnaiger E (2001) Respir Physiol 128:277–297
Gnaiger E (2008) Polarographic oxygen sensors, the oxygraph and high-resolution respirometry to assess mitochondrial function. In Mitochondrial dysfunction in drug-induced toxicity. D.J.a.W. Y, ed. (Wiley), pp. 327–352
Gnaiger E (2009) Int J Biochem Cell Biol 41:1837–1845
Gnaiger E, Kemp RB (1990) Biochim Biophys Acta 1016:328–332
Gnaiger E, Lassnig B, Kuznetsov AV, Margreiter R (1998) Biochim Biophys Acta 1365:249–254
Gnaiger E, Steinlechner-Maran R, Mendez G, Eberl T, Margreiter R (1995) J Bioenerg Biomembr 27:583–596
Gstraunthaler G, Seppi T, Pfaller W (1999) Cell Physiol Biochem 9:150–172
Hatzivassiliou G, Zhao F, Bauer DE, Andreadis C, Shaw AN, Dhanak D, Hingorani SR, Tuveson DA, Thompson CB (2005) Cancer Cell 8:311–321
Hutter E, Renner K, Pfister G, Stockl P, Jansen-Durr P, Gnaiger E (2004) Biochem J 380:919–928
Ishikawa K, Takenaga K, Akimoto M, Koshikawa N, Yamaguchi A, Imanishi H, Nakada K, Honma Y, Hayashi J (2008) Science 320:661–664
Ježek P, Plecitá-Hlavatá L, Smolkova K, Rossignol R (2009) Int J Biochem Cell Biol
John AP (2001) Med Hypotheses 57:429–431
Kim JW, Tchernyshyov I, Semenza GL, Dang CV (2006) Cell Metab 3:177–185
King A, Selak MA, Gottlieb E (2006) Oncogene 25:4675–4682
Kroemer G, Pouyssegur J (2008) Cancer Cell 13:472–482
Liu H, Savaraj N, Priebe W, Lampidis TJ (2002) Biochem Pharmacol 64:1745–1751
Mathupala SP, Rempel A, Pedersen PL (1997) J Bioenerg Biomembr 29:339–343
Moreno-Sanchez R, Rodriguez-Enriquez S, Marin-Hernandez A, Saavedra E (2007) Febs J 274:1393–1418
Nouette-Gaulain K, Bellance N, Prevost B, Passerieux E, Pertuiset C, Galbes O, Smolkova K, Masson F, Miraux S, Delage JP, Letellier T, Rossignol R, Capdevila X, Sztark F (2009) Anesthesiology 110:648–659
Pecina P, Gnaiger E, Zeman J, Pronicka E, Houstek J (2004) Am J Physiol Cell Physiol 287:C1384–1388
Pedersen P (1978) Tumor mitochondria and the bioenergetic of cancer cells. In: Karger S (ed) Progress in experimental tumor research. Basel, New York, pp 190–274
Pedersen PL (2007) J Bioenerg Biomembr 39:211–222
Plecitá-Hlavatá L, Lessard M, Šantorová J, Bewersdorf J, Ježek P (2008) Biochim Biophys Acta 1777:834–846
Pollard PJ, Briere JJ, Alam NA, Barwell J, Barclay E, Wortham NC, Hunt T, Mitchell M, Olpin S, Moat SJ, Hargreaves IP, Heales SJ, Chung YL, Griffiths JR, Dalgleish A, McGrath JA, Gleeson MJ, Hodgson SV, Poulsom R, Rustin P, Tomlinson IP (2005) Hum Mol Genet 14:2231–2239
Reitzer L, Wice B, Kennel D (1979) JBC 254:2669–2676
Rodriguez-Enriquez S, Juarez O, Rodriguez-Zavala JS, Moreno-Sanchez R (2001) Eur J Biochem 268:2512–2519
Rossignol R, Gilkerson R, Aggeler R, Yamagata K, Remington SJ, Capaldi RA (2004) Cancer Res 64:985–993
Simonnet H, Alazard N, Pfeiffer K, Gallou C, Beroud C, Demont J, Bouvier R, Schagger H, Godinot C (2002) Carcinogenesis 23:759–768
Simonnet H, Demont J, Pfeiffer K, Guenaneche L, Bouvier R, Brandt U, Schagger H, Godinot C (2003) Carcinogenesis 24:1461–1466
Steinlechner-Maran R, Eberl T, Kunc M, Margreiter R, Gnaiger E (1996) Am J Physiol 271:C2053–2061
Vaupel P (2008) Oncologist 13(3):21–26
Vaupel P, Hockel M (2000) Int J Oncol 17:869–879
Vaupel P, Hockel M, Mayer A (2007) Antioxid Redox Signal 9:1221–1235
Vaupel P, Mayer A (2005) Effects of anemia and hypoxia on tumor biology. In Anemia in Cancer. European scholl of oncology scientific updates. C. Bokemeyer, and H. Ludwig, eds., pp. 47–54.
Vaupel P, Mayer A, Briest S, Hockel M (2003) Cancer Res 63:7634–7637
Ventura-Clapier R, Garnier A, Veksler V (2008) Cardiovasc Res 79:208–217
Warburg (1930) Metabolisn of tumors. Arnold Constable, London
Willems PH, Smeitink JA, Koopman WJ (2009) Int J Biochem Cell Biol 41:1773–1782
Zu XL, Guppy M (2004) Biochem Biophys Res Commun 313:459–465